Final Report NASA NAG5-7981: Atmospheric Excitation of Planetary Normal Modes

Toshiro Tanimoto

Institute of Crustal Studies, University of California, Santa Barbara, California 93106; email: toshiro@geol.ucsb.edu

KEYWORDS: free oscillation, atmosphere-solid earth coupling, atmospheric turbulence

ABSTRACT: The objectives of this study were to (1) understand the phenomenon of continous free oscillaitons of the Earth and (2) examine the idea of using this phenomenon for planetary seismology. We first describe the results on (1) and present our evaluaitons of the idea (2) in the final section.

In 1997, after almost forty years since the initial attempt by Benioff et al (1959), continuous free oscillations of the Earth were discovered. Spheroidal fundamental modes between 2 and 7 millihertz are excited continuously with acceleration amplitudes of about 0.3–0.5 nanogals. The signal is now commonly found in virtually all data recorded by STS-1 type broadband seismometers at quiet sites. Seasonal variation in amplitude and the existence of two coupled modes between the atmosphere and the solid Earth support that these oscillations are excited by the atmosphere. Stochastic excitation due to atmospheric turbulence is a favored mechanism, providing a good match between theory and data. The atmosphere has ample energy to support this theory because excitation of these modes require only 500–10000 W whereas the atmosphere

contains about 10^{17} W of kinetic energy. An application of this phenomenon includes planetary seismology, because other planets may be oscillating due to atmospheric excitation. The interior structure of planets could be learned by determining the eigenfrequencies in the continuous free oscillations. It is especially attractive to pursue this idea for tectonically quiet planets, since quakes may be too infrequent to be recorded by seismic instruments.

CONTENTS

1 INTRODUCTION

Free oscillations of the Earth provide unique constraints and insights into the Earth's deep interior structure and its dynamics. They are typically observed after a large earthquake, because the Earth starts to oscillate with its resonant frequencies like the clang of a bell. Such a phenomenon was theoretically predicted in the nineteenth century, but unambiguous observation of free oscillations became a reality with the records of the 1960 Chilean earthquake. Theoretical study and preliminary observational study of the free oscillations were apparently becoming popular in the 1950s, though. A year before the 1960 Chilean earthquake, in an article entitled "Searching for the Earth's Free Oscillations", Benioff et al (1959) stated

> "Gilbert and MacDonald (1959) have analysed earthquake records for evidence of the free oscillations. We have taken an opposite approach and analyzed records relatively free of seismic disturbances.... Atmospheric disturbances and non-linear tidal effects must, to some extent, excite the free oscillations even in the absence of earthquakes"

and described an unsuccessful attempt to discover free oscillations from data that were 'relatively free' of seismic signals.

History has shown that the approach by Gilbert & MacDonald (1959), which used earthquake records, has blossomed in the last forty years. Its impact on Earth structure study and earthquake source study has been enormous and is well documented. Clearly, it does not require a repetition by this review. On the other hand, the latter approach of examining seismic records with no obvious evidence of earthquakes seems to have been largely forgotten. The idea may have occurred to some, during the last forty years, that the atmosphere may excite solid Earth oscillations, but such an attempt must have been quickly disregarded as there are virtually no published studies to speak of since Benioff et al's (1959) paper.

In 1997, after almost forty years since the paper by Benioff et al (1959), a possible existence of continuous free oscillations was reported at a meeting in Japan. This work was later published in Nawa et al (1998a). Since then, a few groups of researchers have confirmed the evidence by studying various data sets and, recently, led to evidence that strongly points to the atmosphere as the cause of excitation. This article attempts to summarize recent research activities on this topic.

2 INITIAL DISCOVERY

Nawa et al (1998a) examined a gravimeter record from a superconducting gravimeter at the Showa station in the East Antarctica. The recording period was from 1993 to 1995. They applied a traditional Fourier transformation to each three-day long record and generated a frequency-time spectrogram, specifically targeted to look for the possible existence of continuous modal signals. If there were continuous oscillations, one should be able to follow continuous modal amplitudes throughout this three-year period regardless of the occurrence of earthquakes. They discovered features in the data that suggested such continuous signals and claimed them to be evidence for continuous oscillations.

A gravimeter is sensitive only to spheroidal modes, and Nawa et al (1998a) did indeed observe continuous free oscillations that were spheroidal modes for frequencies between 0.3 and 5 mHz (millihertz). The observed modes were mostly fundamental modes (${}_0S_2$-${}_0S_{43}$) but also contained some overtones (${}_3S_2$ and ${}_1S_4$). These specific features, however, contrast with later observations by other instruments.

Superconducting gravimeters are highly sensitive instruments for tides and long period oscillations of the Earth, but are rarely available because of their cost and high maintenance requirements. Therefore, the number of available stations for such a study is limited. This created a major obstacle when further clarifications and confirmations of the evidence were sought. As a result, after Nawa et al (1998a), other types of records would be examined for understanding the continuous free oscillations, namely two types of data sets. The first is the Lacoste-Romberg gravimeter data from the International Deployment of Accelerometers (IDA) network (Agnew et al 1986). This data set is close to ideal for this analysis because of gravimeter's high sensitivity to low frequency signal and its availability from 1976 to 1995. Suda et al (1998) and Tanimoto et al (1998) analyzed this data set and detected signals of continuous fundamental mode oscillations. The second type of data set that can be used for this problem is the broadband seismometers; in particular, the type of instrument called STS-1 is sensitive to the frequency band below 5 mHz and are widely available (e.g. Wielandt & Streckeisen 1982, Steim 1985, Steim & Wielandt 1985). These studies have been particularly fortunate to have access to an increasing number of permanent seismic stations with the STS-1 instruments since the mid-1980s, which were readily available from Incorporated Research Institutions for Seismology (IRIS) data management center and GEOSCOPE data center (Roult & Montagner 1994). Kobayashi & Nishida (1998) and Tanimoto et al (1998) analyzed this type of data and detected the same modal signal from the continuous free oscillations.

Various studies, based on both the IDA gravimeters and the broadband seismic instruments (STS-1), have yielded consistent results; the observed signals were spheroidal modes for frequencies between 2 and 7 mHz. Signals below 2 mHz or above 7 mHz were not observed. All the observed modes were fundamental modes, ranging from ${}_0S_{15}$ to ${}_0S_{60}$. Modal amplitudes for these modes were fairly constant, in unit of acceleration, and were approximately 0.3–0.5 ngal (nanogal).

There were major differences between the initial result based on the superconducting gravimeter (Nawa et al 1998a) and the subsquent results based on the IDA gravimeter and the STS-1 results (Kobayashi & Nishida 1998, Tanimoto et al 1998). Primarily, fundamental mode observation was confined to frequencies between 2 and 7 mHz. This makes quite a contrast with Nawa et al (1998a), which showed signals down to about 0.3 mHz, meaning it extended to the frequency band of some of the gravest modes such as ${}_0S_2$ and ${}_0S_3$. In the IDA or the STS-1 records, such a low frequency band is dominated by noise, which dramatically increases below 2 mHz. Secondly, overtones (${}_3S_2$ and ${}_1S_4$, both at about 1 mHz) were identified in the superconducting gravimeter data, but there was absolutely no signal from overtones in the IDA and STS-1 records.

The reason for this discrepancy is not currently clear. There were some doubts raised against the quality of superconducting gravimeter data at Showa station (Imanishi 1998), but further examination (Nawa et al 1998b), including other superconducting gravimeter data, seemed to indicate that the results in the initial study were sound. The reason for these discrepancies may be due to differences in the noise behavior of instruments, because noise below 2 mHz at Showa station seems much lower than noise in the IDA and STS-1 instruments (Nawa et al, 1998b). This explanation does not seem to entirely explain the variations in results, because noise characteristics at Showa station seem different from other sites such as Matsushiro (Japan), which is another superconducting gravimeter location. It will probably require much more elaborate study to understand these discrepancies; this review will not go into any additional detail. It is clear that comparative study of superconducting gravimeters and other instruments is clearly called for, but is hard to perform at present because of the low availability of superconducting data.

Since 1998, most of the progress on continuous free oscillations were made with the analysis of the IDA data and the STS-1 broadband seismometer data. Of the two, the main source of data has been the STS-1 data, because the IDA network stopped its data collection in 1995. Because of this situation, in this review, I will hereafter focus on the results and analysis of the STS-1 broadband seismometers.

3 EARTHQUAKES ARE NOT THE CAUSE

Because the work by Benioff et al (1959) was largely forgotten in 1998, the notion of the existence of continuous, background free oscillations was not accepted easily when we tried to publish our papers. There were three typical questions:

1. Since large earthquakes generate great-circle surface waves, are these modal peaks simply great-circling waves that are spawned by occasional large earthquakes?
2. Are they really continuous?
3. Are they not generated by cumulative effect of small earthquakes?

For all questions, some careful analyzes were carried out.

3.1 Not Large Earthquakes

The first question is relatively easy to answer. Nawa et al (1998a) and Suda et al (1998) generated synthetic seismograms for the earthquakes in the Harvard moment tensor catalog and compared the synthetic spectra with the observed spectral data. The Harvard moment tensor catalogue is an almost complete catalogue for earthquakes larger than magnitude 5.5. There have been some reports of missing events in the catalogue (e.g. Shearer 1994), but such an omission is rare and is not likely to create problems in the analysis.

The results in the above two studies indicated that synthetic spectra could not create peaks as high as those observed in data. This result supports strongly that these spectral peaks were not generated by large earthquakes.

This can be understood as a strong effect of attenuation on seismic waves. Energy loss of the great-circling surface waves due to attenuation should cause the amplitude to decay to a 4-5 percent level after one day, assuming a period 300 seconds and Q of 300. Since magnitude-6 earthquakes only occur every three days on average, effects of large earthquakes are not likely to sustain the level of modal amplitudes observed in data.

3.2 Continuity of Modal Signal

In order to examine the continuity of free-oscillation signals, Tanimoto et al (1998) adopted the following approach; if the oscillations were continuous, the modal signal should exist for the time interval during which no significant earthquakes were reported. Using the earthquake catalogue and visual examination of seismograms, dates with no hint of seismic signal were selected. These selected days were called *seismically quiet* days. Of course, strictly speaking, there are no earthquake-free days; there must be small earthquakes that happen somewhere in the Earth everyday. But if these earthquakes were small, they would not generate long period oscillations efficiently. For example, if an earthquake is smaller than magnitude 5, it would generate modal signals much smaller than the observed amplitudes.

Figure 1 shows an example of spectra from selected days at station Harvard (HRV), located in the eastern United States. This figure shows stacked spectral amplitudes from about 100 seismically quiet days. The top figure shows spectra between 1 and 10 mHz, and the bottom figure shows an enlarged portion of the above figure between 3 and 6 mHz. Vertical lines indicate fundamental mode eigenfrequencies of preliminary reference earth model (PREM) (Dziewonski & Anderson 1981). The enlarged figure at the bottom clearly shows that all peaks in the frequency range match spheroidal fundamental mode frequencies. Basically every peak is related to a fundamental mode multiplet (each peak actually contains $2l + 1$ modes, where l is the angular degree). Data from other stations indicated that this match occurs over a slightly wider frequency range, approximately ranging from 2 to 7 mHz. The same feature can now be found at virtually all low noise sites with STS-1 broadband seismometers.

The stacked spectral amplitudes in Figure 1 do not directly prove that the signal is continuous. Continuity of signal is confirmed in Figure 2 (see color insert), which shows the narrow frequency band data (3–4 mHz) at a Hawaiian station Kipapa (KIP), from 1989 to 1991. In this figure, spectral amplitudes of acceleration from each day over three years are plotted vertically with three colors; blue, yellow, and red denote amplitudes of acceleration below 0.4 ngal, between 0.4 and 2 ngal, and above 2 ngal, respectively. Arrows on the lefthand side of the figure denote the spheroidal mode eigenfrequencies of the PREM from ${}_0S_{22}$ to ${}_0S_{32}$. It should be noted that all yellow horizontal stripes are almost exactly at the eigenfrequencies of fundamental spheroidal modes. Occasional vertical red lines correspond to the occurrence of large earthquakes and their aftershocks, which tend to bury the yellow stripes temporarily for a period of about a week because of aftershock occurrence. Despite these interruptions, however, yellow horizontal stripes can be continuously observed through the years and suggest that they exist irrespective of earthquake occurrence. These yellow lines represent concrete evidence for continuously excited spheroidal modes.

3.3 Not Small Earthquakes

The third question that small earthquakes may be exciting the continuous oscillations appears to be a very plausible hypothesis. This question has been analyzed from various angles.

The first approach is an extension of the synthetic seismogram approach. Suda et al (1998) extended their synthetic-seismogram approach into the lower magnitude threshold by assuming a Gutenberg-Richter magnitude-frequency relation (hereafter G-R relation), for the number of small events, and the Poisson distribution for temporal variations (earthquake occurrence). With these assumptions, they extended the magnitude threshold from 5.5 down to 4.6 and created the synthetic spectra. Results showed that spectral amplitudes in synthetic spectra were much smaller than those in the data, thereby concluding that a cumulative contribution of small earthquakes could not create the observed modal amplitudes.

The same conclusion was reached by Tanimoto et al (1998) using a simple order-of-magnitude argument. If the number of earthquakes obeys the G-R relation, there are ten times more events for a decrease of magnitude by one. On the other hand, amplitude in the frequency band 2–7 mHz is proportional to the moment of earthquakes. The magnitude-moment relation is such that an amplitude decrease is about 1/30 for a decrease of magnitude by one. If each small event contributes randomly, the combined effect is $\sqrt{10} \times 1/30 \approx 1/10$ from events one magnitude below the cutoff. The cumulative effect from all small events will then be $1/10 + 1/10^2 + \cdots = 1/9$, resulting in only a 1/9 contribution from a lower limit magnitude cutoff. Clearly, this is much too small to be significant.

The third set of evidence against the hypothesis of small earthquakes is purely observational. It turns out that there was a special characteristic in the amplitude behavior of the observed modes that indicated that the modes were not related to ordinary earthquakes. Figure 3 shows a plot of modal amplitude of ${}_0S_{26}$ against the moment of each day. Cumulative moment is used for this plot, which means if there was more than one earthquake, the sum of the moments from all the events in the same day was used for the abscissa. Raw data are plotted in the bottom panel and the median and variance (L1 norm) are shown in the top panel. For days with earthquakes larger than 10^{18} (Newton-meter or Nm), there is clearly a linearly increasing trend in the data. The linear range is approximately from 10^{18} to 10^{21} Nm. The dash line is drawn as a reference and is given by

$$A = \frac{100(ngal)}{10^{21}} M_o, \qquad (1)$$

where A is the acceleration spectral amplitude and M_o is the moment in Nm. For an earthquake of magnitude 8, the moment is 10^{21} Nm, and the modal amplitude of ${}_0S_{26}$ is $A = 100$ ngal.

One of the most notable features in Figure 3 is the flattening trend below 10^{18} Nm. There is a break in trend below and above this moment. This figure shows that the flattening trend continues down to 5×10^{16} Nm, which is the lowest cutoff in the Harvard moment tensor catalogue. But this constant amplitude continues at the same (constant) level for days without any reported earthquakes. This constant amplitude means that, regardless of the size of earthquakes, as long as earthquakes are below 10^{18} Nm, this mode (${}_0S_{26}$) is excited at about the same amplitude level. Only when an earthquake larger than moment 10^{18} Nm occurs, do modal amplitudes become proportional to the moment. Earthquakes below the moment 10^{18} Nm do not excite this mode above this constant amplitude. This constancy in amplitude for events below 10^{18} Nm is hard to explain by the cumulative effects of small earthquakes. This evidence clearly suggests that a different mechanism controls these modal amplitudes above and below the threshold moment of 10^{18} Nm.

In summary, there are three independent arguments against the cumulative effect of small earthquakes; (*a*) synthetic seismogram approach, (*b*) order of magnitude analysis and (*c*) constancy in observed amplitudes on days of small earthquakes. The essential point is that it would require a large deviation from the Gutenberg-Richter's magnitude-frequency relation in order to produce the observed, constant amplitude behavior. Therefore, it is very unlikely that small earthquakes are the cause of continuous free oscillations.

4 SEASONAL VARIATION IN AMPLITUDE

The arguments in the above section are fairly strong, but some skeptical people still expressed that it was hard to believe that such free oscillations are not related to earthquakes. However, the critical evidence came from the observation of seasonal variations in the data. There were two aspects in the observations of seasonal variations. The first is the seasonal variations in modal amplitudes; stacked modes clearly exhibited seasonal variations in amplitudes (Tanimoto & Um 1999, Nishida et al 2000). The second is an existence of coupled modes between the atmosphere and the solid Earth (Nishida et al 2000).

The existence of seasonal variation indicates that a source is not earthquake-related. It also indicates that the source is not in the solid Earth, because seasonality is usually not found in solid Earth processes and points either to an atmospheric process or an oceanic process as its cause. Furthermore, a hint of the existence of coupled modes strongly suggests that the atmosphere, rather than the ocean, is the cause of continuous free oscillations.

4.1 Seasonality in Stacked Amplitude

Because the level of the signal is marginal, seasonal variations were not found in raw data; its detection required some form of stacking in order to enhanse the signal to noise ratio. Figure 4 shows stacked modal amplitude data from Kunming (KMI), a very quiet Chinese station, for the time interval from 1988 to 1996. The spectral amplitudes at modal frequencies of 21 modes (${}_0S_{20}$-${}_0S_{40}$) were averaged for each day and plotted by solid circles. Noise was also estimated by selecting the amplitudes halfway between adjacent modes. Open circles in the figure denote this result for each day and are regarded as an estimate for noise.

The analysis focuses on the concentrated points near the bottom of Figure 4 with approximate Gaussian distributions, because these points correspond to data from seismically quiet days. The figure shows that solid circles are systematically larger than open circles, which is more evidence for the continuously excited modes (Figure 1). Points with large amplitudes are mostly caused by seismic signals from (distant) earthquakes; typically, earthquake signals are much larger than the maximum in this figure (2 ngal) but occasionally they are below 2 ngal and show up in this plot.

Selecting 15 quiet sites similar to this station (KMI), stacked amplitude data from the bell-shaped, small amplitude region were binned according to months. Figure 5 shows the results of monthly averages, and clearly shows biannual variations, with a peak in December-January-February and another peak in June-July-August.

The results by Nishida et al (2000) also demonstrated seasonal variations which lent independent support to the observed amplitudes containing seasonality. But there are some differences between the two observations, particularly in the periodicity in the data; the periodicity reported in Nishida et al (2000) is annual variation while Tanimoto & Um (1999) reported biannual variation. This difference seems to be related to a slightly different data analysis procedure in the two studies. The difference is in the way the signal and noise were handled. In short, Nishida et al (2000) subtracted noise from signal by assuming a Gaussian distribution of noise whereas Tanimoto & Um (1999) did not perform such a subtraction procedure. There is a hint in some of the data that suggests this simple difference in analysis can lead to the reported differences; Figure 6 shows the variations in the modal amplitudes (signal) and noise for the station KMI. Data from an eight-year long period were used to retrieve this result. All stacked modal data were binned into months, and monthly averages were estimated. It should be noted that modal peaks show biannual variations (Figure 6, *top trace*), whereas noise clearly shows annual variations with a single peak in December-January-February (Figure 6, *bottom trace*). Subtraction of noise from signal would reduce amplitudes in December-January-February while enhancing them in June-July-August. Therefore, this simple subtraction procedure appears to be the cause of differences in the two studies.

Clearly, further study is required to clarify this point. Virtually all simple stack results (without noise subtraction) show two peaks in a year while noise subtraction tends to stress one of the peaks in June-July-August. Therefore, we suspect that both periodicities are contained in the data. It seems more important to recognize at this stage, however, that seasonal variations do exist in modal amplitude data.

4.2 Coupled Modes Between Atmosphere and Solid Earth

Some of the most intriguing evidence for the coupling between the atmosphere and the solid Earth was presented by Nishida et al (2000). They pointed out that two modes, ${}_0S_{29}$ and ${}_0S_{37}$, show significantly larger amplitudes than other modes in the stacked records.

These two modes happen to be at the same frequencies as the Rayleigh waves, originally pointed out by Kanamori & Mori (1992) and Widmer & Zürn (1992) in the seismic records of the Mt. Pinatubo volcanic eruption. Both studies showed that Rayleigh waves at two periods, one at 230 s and the other at 270 s, were preferentially excited after the volcanic eruption due to resonance between the atmosphere and the solid Earth. Rayleigh waves at these periods are equivalent to the spheroidal fundamental modes ${}_0S_{29}$ and ${}_0S_{37}$. This phenomenon occurs because proximity of resonance periods between the solid Earth modes and the atmospheric modes makes the two media vibrate together; or viewed from the coupled system between the atmosphere and the solid Earth, these are the modes of such a coupled solid earth-atmosphere system. Existence of such a coupled mode was also supported in theoretical analyses by Watada (1995) and Lognonné et al (1998).

This evidence has only been confirmed by one study and, clearly, further examination is required to establish it as firmer evidence. It is a critically important point because this observation removes oceanic processes as a possible cause of excitation.

5 ATMOSPHERIC EXCITATION MECHANISM

Observational evidence clearly points to the atmosphere as a source of excitation of the continuous free oscillations. The next question is, how does the atmosphere excite the oscillations of the Earth? What kind of mechanism is working to excite these modes? And is the energy in the atmosphere sufficient to generate such solid Earth oscillations?

The last question, basically a question of energetics, will be discussed in the section below. In this section, we will describe a hypothesis of stochastic normal mode excitation by the atmosphere that provides an answer to the first two questions. This hypothesis was proposed and developed over the last few years (Kobayashi & Nishida 1998, Tanimoto 1999, Tanimoto & Um 1999, Fukao et al 2001) and, so far, is the only hypothesis that can be tested quantitatively. We mainly summarize the approach developed by Tanimoto (1999) and Tanimoto & Um (1999).

Obviously, it is difficult to pinpoint the detailed process of atmospheric excitation mechanism at this stage. However, there are certain characteristics of the atmosphere that help narrow down the potential processes. For example, it seems safe to state that the mechanism must involve atmospheric turbulence, because one of the most important properties of the atmosphere for the frequency range of observation (2–7 mHz) is turbulence. It is obvious that, in order to excite free oscillations, the atmosphere must supply energy in this frequency band. Therefore, the excitation mechanism must involve a transfer of energy from atmospheric turbulence to the solid Earth oscillations.

One of the hallmarks of turbulence is its stochastic nature. Forcing on the solid Earth is thus random, not only in space but also in time. Excitation of free oscillations under such a condition was formulated (Tanimoto, 1999), following the work done by Gilbert (1971) for the Earth and Goldreich & Keeley (1977) for the Sun. The basic idea can be sketched briefly as follows; let us denote the displacement excited by a stochastic force by $u_i(t)$. Using the normal mode theory, $u_i(t)$ can be written as a sum of normal modes as

$$u_i(t) = \sum_n a_n(t) u_i^{(n)}, \tag{2}$$

where $a_n(t)$ is the excitation coefficient for the nth normal mode and is to be determined by the theory. Functions $u_i^{(n)}$ $(n = 0, 1, 2, ...)$ are the eigenfunctions and form a complete set of basis functions to expand the displacement field.

If a global stochastic force is applied at the surface of the Earth, the excitation coefficient can be written by

$$\begin{aligned} < | \quad a_n \quad |^2 >= & \frac{R^4}{I_n^2} \int_S d\Omega' \int_S d\Omega'' \int_{-\infty}^{t} dt' \int_{-\infty}^{t} dt'' \\ & \times u_i^{(n)}(\Omega') u_i^{(n)}(\Omega'') \exp\{-\frac{\omega_n(2t - t' - t'')}{2Q_n}\} \\ & \times \frac{\sin\omega_n(t-t')\sin\omega_n(t-t'')}{\omega_n^2} \\ & \times < f(t', \Omega') f(t'', \Omega'') >, \end{aligned} \tag{3}$$

where R is the radius of the Earth, I_n is the normalization of an eigenfunction, Ω' and Ω'' are the spatial integration variables on the surface of the Earth, and t' and t'' are the time integration variables. Q_n is the attenuation parameter for the nth mode, ω_n is its eigenfrequency, and the force (pressure) correlation

$< f(t', V')f(t'', V'') >$ is the source of excitation.

The above equation is a general formula for a stochastic force denoted by $< f(t', V')f(t'', V'') >$. For the specific problem of atmospheric excitation, we must retrieve temporal and spatial characteristics of forcing from the atmospheric data and express this term by the derived properties. Let us assume that atmospheric surface pressure fluctuation is the cause of excitation. Then, specific quantities required to express this forcing term consist of the following three quantities: (i) power of pressure variations, (ii) temporal correlation, and (iii) spatial correlation. In a mathematical expression, this can be written as a function of wavelengths (e.g. Goldreich & Keeley 1977):

$$< f(t', \Omega')f(t'', \Omega'') >= \int_0^\infty \frac{d\lambda}{\lambda} P_\lambda(\Omega', \Omega'')G_\lambda(t', t'')H_\lambda(\Omega', \Omega''), \tag{4}$$

where the integration is with respect to wavelength. The above three quantities are, respectively, P_λ, the power of pressure variation; $G_\lambda(t', t'')$, the temporal correlation function; and $H_\lambda(\Omega', \Omega'')$, the spatial correlation function.

P_λ can be estimated, in principle, from surface atmospheric pressure fluctuations. This was fairly straightforward and the estimates were quite robust, as surface pressures do not vary very much globally provided that a long temporal ensemble (over a few months) was taken (Tanimoto & Um 1999). At all stations examined, pressure showed a $1/f$ functional dependence, where f is the frequency, and the amplitudes were similar from station to station after altitude corrections. The more uncertain quantities were the temporal and spatial correlations; the spatial correlation should be 10 km or less because the scale height of the atmosphere is about 10 km, and eddies in three-dimensional turbulence should have similar vertical and horizontal length scales. The temporal correlation was inferred from the scaling laws for the characteristic size of eddies and for the velocities as a function of wavelength (Landau & Lifshitz 1987, Frisch 1995, Tennekes & Lumley 1972). It is clear that these estimates are crude and must be examined in the future.

The integral in Equation 4 can be evaluated analytically by assuming certain functional forms of $G_\lambda(t', t'')$ and $H_\lambda(\Omega', \Omega'')$ (Tanimoto & Um 1999). Because the data are vertical component seismograms and are given in units of acceleration, the formula for the vertical acceleration is useful and is written by:

$$\begin{aligned} A_n &= \omega^2 \sqrt{< |a_n|^2 >} U_n(R) \\ &= 1292 \frac{\sqrt{Q_n} R H_s P_H}{(\omega_n \tau_H)^{5/2} M_n} \sqrt{\frac{k_\Omega}{k_\tau^5}} F(\frac{\omega^2 \tau_H^2 k_\tau^2}{100}), \end{aligned} \tag{5}$$

where ω_n is the eigenfrequnecy of the $n-th$ mode, τ_H is the period of energy bearing eddy, and k_τ and k_Ω are sensitivity parameters that should be close to unity but are varied in the numerical evaluations. M_n is the modal mass and is defined in this review by

$$\frac{1}{M_n} = \frac{\sqrt{U_n(R)^2 + l(l+1)V_n(R)^2} U_n(R)}{\int_E \rho_s \{U_n(r)^2 + l(l+1)V_n(r)^2\} r^2 dr}. \tag{6}$$

U_n and V_n are the vertical and horizontal eigenfunctions of a spheroidal mode [e.g. Aki & Richards 1980].

Because the theory contains some uncertain parameters, there is not much merit in attempting to fit the spectral amplitude data exactly. Instead, I computed theoretical predictions with various parameter ranges and sought a range with good fit. In evaluating Equation 3, except for the three parameters I vary, the scale height of the atmosphere was fixed at $H_s = 8.7$ km, the Earth's radius at $R = 6371$ km, pressure variations P_H were computed by $P = 0.32/f$, and modal parameters (eigenfrequency ω_n, its modal mass M_n, and its attenuation parameter Q_n) fixed to those of the standard Earth model PREM.

Figure 7 shows three plots, each of which contains three different cases of theoretical predictions. From top to bottom, k_τ is held at 1.0 ($k_\tau = 1.0$) and $1/\tau_H$ is varied as $1/\tau_H = 1.0$ mHz (*top*), 1.5 mHz (*middle*), and 2.0 mHz (*bottom*). In each panel, three cases of k_Ω are given by a solid line, a short-dashed line, and a long-dashed line, the values being $k_\Omega = 1$, 2, and 4. In all cases the smaller the k_Ω, the smaller the acceleration amplitude. The observed modal amplitudes from seventeen stations are plotted by circles.

The match between theory and data is generally good in these plots, particularly in the bottom panel. They demonstrate that atmospheric pressure variations at the surface are capable of exciting solid Earth normal modes up to the level of observed amplitudes. They also suggest that, in order to fit the overall frequency trend in the data, the frequency of energy-containing eddies ($1/\tau_H$) should be close to 2 mHz.

The main point in this theoretical exercise is that the stochastic atmospheric excitation can explain observed amplitudes of continuously excited normal modes. Even though the atmospheric force tends to be underestimated by solid Earth scientists, the atmospheric turbulence seems to be sufficiently vigorous to excite the oscillations of the Earth.

6 ENERGETICS

The proposed stochastic excitation process in the section above is not necessarily an efficient process. One may wonder if such an inefficient excitation mechanism can ever explain, energetically, the observed modal amplitudes. But such a concern does not seem relevant if the abundant energy in the atmosphere is recognized.

First, let us consider the energy available in the atmosphere. If we restrict our consideration to the kinetic energy in the atmosphere, the integrated energy over the globe reaches about $10^{16} - -10^{17}$ W (e.g. Peixoto & Oort 1992). This is a large fraction of radiated energy from the Sun because the solar radiation is about 1.2×10^{17} W, including consideration for albedo.

On the other hand, the required energy for the background oscillations is only 500–10000 W; the lower limit comes from an estimate that asked, "What is required to compensate for the loss of energy by attenuation of each mode ?". All the fundamental modes in the frequency band 2–7 mHz are included in the estimate, and the total energy is only about 500 W.

The upper limit comes from an estimate that asked, "“What is the energy required to excite these modes from zero amplitude to the observed level of 0.4 ngal ¿‘" This upper estimate is made because all observed modes are not necessarily coherent. If all oscillations were coherent, the lower limit of 500 W is sufficient to maintain the oscillations. But even if all modes were excited anew, the upper limit of the total energy of oscillations would only amount to 10000 W.

This detailed discussion seems pointless if the differences in magnitude of energy between the atmospheric kinetic energy and the solid Earth oscillations is recognized; there is basically a difference of more than ten orders of magnitude because one is about 10^{16--17} W whereas the other is at most 10^4 W. Inefficiency in the excitation process hardly seems to matter for these two disparate values; there is no question that the atmosphere has ample energy to excite continuous free oscillations.

7 APPLICATION TO PLANETARY SEISMOLOGY

One of the motivations for the study of continuous free oscillations is its potential application to planetary seismology (Kobayashi & Nishida 1998, Tanimoto et al 1998). For the Earth, continuous free oscillations do not provide any new information about its interior structure. We already know the structure and its eigenfrequencies and eigenfunctions. But if continuous free oscillations were detected in another planet, the observed frequencies would provide new information about the interior structure of that planet.

This idea may be especially attractive on a tectonically quiet planet such as Mars. Seismicity estimates for Mars indicate that the level of seismic (tectonic) activity is likely to be about three orders of magnitude lower than that on the Earth (Golombek et al 1992). In addition, the search for short period seismic signals for P-waves and S-waves, generated by Mars quakes, may not provide fruitful results. But if the atmosphere is causing the continuous free oscillations, eigenfrequencies in Mars may be determined by installing suitable seismometers on the surface for some periods of time. The observed eigenfrequencies will in turn provide information about the interior of Mars. Estimate of such effects can be made with Equation 5. Roughly speaking, the ratio of modal amplitudes at the same frequency between Earth and Mars will be given by

$$\frac{A_M}{A_E} = \frac{H_M}{H_E}\frac{R_M}{R_E}\frac{\rho_M}{\rho_E}\left(\frac{\tau_M}{\tau_E}\right)^{5/2}\frac{M_E}{M_M}, \tag{7}$$

where H, R, ρ, τ, and M are the scale height of atmosphere, the radius, average density, the characteristic overturn time of the atmosphere and the modal mass, respectively. The subscripts M and E refer to those quantities for Mars and for Earth, respectively. Computation of the modal mass (Equation 6) requires the eigenfunctions of each spheroidal fundamental mode, for which one of the most recent model by Sohl & Spohn (1997) was used. There are obviously large uncertainties in this model but, for the purpose of making crude estimates, this model is sufficient. Other assumed constants are given in Table 1.

This estimate of relative amplitudes for the spheroidal modes between Mars and Earth are shown in Figure 8 (and the bottom row of Table 1). There is an increasing trend in amplitude with frequency, because Mars is smaller in size and thus relatively larger amplitudes are expected for higher frequency modes. In general the expected amplitudes for Mars are about 30–50 percent of those observed in the Earth and they are not likely to reach the level of amplitude observed in the Earth, at least for frequencies below 10 mHz.

My overall assessment of this result is that observation of continuously excited modes in Mars may be technically hard. Considering the fact that continuous oscillations are observed only at quiet sites in the Earth, the expected amplitudes at the 30–50 percent level may be too small. If one can stack data from many stations, one may be able to overcome this difficulty, but the available observation time and the number of stations for Mars are likely to be limited. My estimate is admittedly crude and could be off even an order of magnitude, but in general, this result indicates potentially huge obstacles in applying the new concept on Mars. However, the idea may work for other planets.

8 SUMMARY

In 1997, after almost forty years since the initial attempt by Benioff et al (1959), continuous free oscillations of the Earth were discovered. The study of these oscillations over the last few years can be summarized as follows:

- Earth is constantly shaking by spheroidal fundamental modes between 2 and 7 millihertz (from ${}_0S_{15}$ to ${}_0S_{60}$). Modal amplitudes are approximately constant in acceleration and are about 0.3–0.5 nanogals.

- Overtones were not seen in IDA gravimeter data and the broadband seismometers (STS-1). All observed modes are spheroidal fundamental modes.

- They are clearly not related to occurrence of large earthquakes (magnitude larger than 5.5). The cumulative effects of small earthquakes also cannot explain the observed amplitudes quantitatively.

- Seasonal variations are seen in stacked modal amplitudes. Also, there is a hint of existence of coupled modes between the atmosphere and the solid Earth. These observations point to the atmosphere as the cause of continuous free oscillations.

- Stochastic excitation of normal modes by surface pressure variations, caused by atmospheric turbulence, can explain the overall amplitudes of observed modes. In terms of the energetics, the atmosphere contains ample energy for excitation of continuous free oscillations.

- This phenomenon provides a new concept in planetary seismology. If a similar mechanism were to occur on other planets, free oscillations may be observed by installing suitable seismometers on the surface of the planet for some period of time. This may be particularly attractive for some planets, since the mechanism works even if a planet is tectonically dead. However, the estimated amplitudes for Mars is about half of those found in the Earth. Therefore, at least for Mars, this idea may not be practical after all.

Literature Cited

Aki K, Richards PG. *Quantitative Seismology: Theory and Methods*, W. H. Freeman, New York, 1980, 932pp.

Agnew, DC, Berger J, Farrell W, Gilbert JF, Masters G, Miller D. 1986. Project IDA: A decade in review. *Eos, Trans. AGU*, 67:203–212.

Benioff H, Harrison JC, LaCoste L, Munk WH, Slichter LB. 1959. Searching for the Earth's free oscillations, *J. Geophys. Res.*, 64:1334–37.

Dziewonski AM, Anderson, DL. 1981. Preliminary reference Earth model, *Phys. Earth Planet. Inter.* 25:297–356.

Frisch, U. 1995. *Turbulence*, Cambridge Unievrsity Press, New York, 296pp.

Fukao Y, Nishida K, Suda N, Nawa K, Kobayashi N. A theory of the Earth's background free oscillations, *J. Geophys. Res.*, in press.

Gilbert F. 1971. Excitation of normal modes of the earth by earthquake sources, *Geophys. J. R. Astron. Soc.* 22:223–226.

Gilbert F, MacDonald G. 1959. Free oscillations of the earth, *J. Geophys. Res.* 64:1103–1104.

Goldreich P, Keeley DA. 1977. Solar seismology, II, The stochastic excitation of the solar p-modes by turbulent convection, *Astrophys. J.* 212:243–251.

Golombek M, Banerdt W, Tanaka K, Tralli D. 1992. A prediction of Mars seismicity from surface faulting, *Science* 258:979–981.

Imanishi Y. 1998. Commnet on "Incessant excitation of the Earth's free oscillations" by Nawa et al *Earth, Planets and Space* 50:883–885.

Kanamori H, Mori J. 1992. Harmonic excitation of mantle Rayleigh waves by the 1991 eruption of Mount Pinatubo, *Geophys. Res. Lett.* 19:721-724.

Kobayashi N, Nishida K. 1998. Continuous excitation of planetary free oscillations by atmospheric disturbances. *Nature* 395:357–360.

Landau LD, Lifshitz EM. 1987. *Fluid Mechanics, Course Theor. phys.*, vol. 6, 2nd ed., Pergamon Press, New York, 536pp.

Lognonné P, Clevede E, Kanamori H. 1998. Computation of seismograms and atmospheric oscillations by normal mode summation for a spherical Earth model with realistic atmosphere.

Geophys. J. Int. 135:388–406.

Nawa K, Suda N, Fukao Y, Sato Y, Aoyama Y, Shibuya K. 1998a. Incessant excitation of the Earth's free oscillations. *Earth, Planets and Space* 50:3–8.

Nawa K, Suda, N, Fukao Y, Sato T, Aoyama Y, Shibuya K. 1998b. Reply. *Earth, Planets and Space* 50:887–892.

Nishida K, Kobayashi N, Fukao Y. 2000. Resonant oscillations between the solid Earth and the atmosphere. *Science* 287:2244–2246.

Peixoto J, Oort AH. 1992. *Physics of Climate*, Springer-Verlag, New York, 520pp.

Roult G, Montagner JP. 1994. The Geoscope program, *Ann. Geofis.* 37:1054–1059.

Shearer PM. 1994. Global seismic event detection using a matched filter on long-period seismograms, *J. Geophys. Res.* 99:13713–13725.

Sohl F, Spohn T. 1997. The interior strcuture of Mars: Implications from SNC meteorites, *J. Geophys. Res.* 102:1613–1635.

Steim JM. 1985. *The very broad band seismograph*, Ph. D. Thesis, Harvard University, Cambridge, Massachsetts.

Steim JM, Wielandt E. 1985. The very broad band seismograph; Part 2: Station processor (abstract), *EOS, Trans. Am. Geophys. Un.* 66:312.

Suda N, Nawa K, Fukao Y. 1998. Earth's background free oscillations. *Science* 279:2089-2091.

Tanimoto T. 1999. Excitation of normal modes by atmospheric turbulence, *Geophys. J. Int.* 136:395–402.

Tanimoto T, Um J, Nishida K, Kobayashi N. 1998. Earth's continuous oscillations observed on seismically quiet days. *Geophys. Res. Lett.* 25:1553–1556.

Tanimoto T, Um J. 1999. Cause of continuous oscillations of the Earth, *J. Geophys. Res.* 104:28723–28739.

Tennekes H, Lumley JL. 1972. *A First Course in Turbulence*, MIT Press, Cambridge, Mass.

Watada S. 1995. Near-source acoustic coupling between the atmosphere and the solid earth during volcanic eruption, Ph.D. dissertation, Caltech.

Widmer R, Zürn W. 1992. Bichromatic excitation of long-period Rayleigh and air waves by the Mount Pinatubo and El Chichon volcanic eruptions, *Geophys. Res. Lett.* 19:765–768.

Wielandt E, Streckeisen G. 1982. The leaf-spring seismometer:design and performance, *Bull.*

Seismol. Soc. Am. 72:2349–2367.

Figure Caption

Table 1: Amplitude Estimate

	Earth	Mars
Atmospheric density (kg/m^3)	1.2	0.019
Radius (km)	6371	3390
Surface g (m/s^2)	9.8	3.7
Scale height of atmosphere (m)	8700	12100
Relative pressure	1	0.006
Char. overturn time for the alrgest eddy (s)	2100	1060
Solar energy flux (W/m^2)	1370	590
Albedo	0.30	0.15
Relative modal amplitude	1	0.3-0.5

Figure 1: Stacked spectra from seismically quiet days at station Harvard (HRV) for frequencies between 1 mHz and 10 mHz (*top*) and an enlarged figure between 3 mHz and 6 mHz (*bottom*). All spectral peaks between 3 and 6 mHz correspond to spheroidal modes. Vertical lines are drawn at the eigenfrequencies of spheroidal fundamental modes for the preliminary reference Earth model (PREM). These peaks exist continuously, irrespective of earthquake occurrence.

Figure 2: Spectral amplitude at Kipapa (KIP) for frequencies between 3 mHz and 4 mHz during the period between 1989 and 1991. For each day, there is a vertical line. Three different colors, blue, yellow, and red, denote three different levels of amplitudes, and indicate amplitudes less than 0.4 nGal, between 0.4 and 2 nGal, and larger than 2 nGal, respectively. On days of large earthquakes and their subsequent few days, vertical red lines appear. The arrows on the lefthand side of the figure indicate the eigenfrequencies of fundamental spheroidal modes of the preliminary reference Earth model (PREM). Angular degrees of modes are from 22 to 32. Yellow horizontal stripes are seen at the eigenfrequencies of modes and indicate that they are continuously excited modes.

Figure 3: Amplitudes of ${}_0S_{26}$ at Kipapa (KIP) are plotted against the cumulative moment of each day. Raw data are shown at bottom. The top panel shows the median and variance (L1 norm) estimated from the raw data. Data with earthquakes larger than 10^{18} Nm show linear trend; this is because low-frequency modal amplitudes are proportional to moment. This trend is approximated by a dashed line. Amplitudes of this mode become flat for earthquakes below about 10^{18} Nm, which cannot be explained easily by cumulative effect of small earthquakes.

Figure 4: Average modal amplitudes for modes between ${}_0S_{20}$ and ${}_0S_{40}$ are computed everyday from 1988 to 1996 at station Kunming (KMI). Plotted results are from quiet days because amplitudes at days of large earthquakes (magnitude larger than about 6) usually far exceed 2 ngals, the maximum amplitude plotted in this figure. Solid circles are amplitudes of mode eigenfrequencies (signal) and open circles are noise estimated from points halfway between adjacent modal peaks. The fact that solid circles are systematically higher means that these modes are always excited. Statistical distributions are shown at right.

Figure 5: Monthly averages of modal amplitudes in Figure 4 are plotted. Seasonal variations are seen clearly with two peaks, one in December-January-February and the other in June-July-August.

Figure 6: At Kunming (KMI), biannual variations of modal signal (*top*) and annual variations of noise are clearly seen. If noise were subtracted from signal, the results would be dominated by a peak in December-January-February. At most stations, straightforward stacking produces biannual variations as in the top trace.

Figure 7: Comparison between theory and data. Three different cases of k_τ and τ_H are compared with modal amplitude data (*solid circles*). In each panel, three curves correspond to different values of k_Ω (1,2, and 4). The best fit is achieved by the bottom panel, which has the energy-containing eddy at frequency 2 mHz. It is important that stochastic atmospheric pressure fluctuation can generate 0.2-0.4 ngal of modal amplitudes and supports the atmospheric excitation hypothesis.

Figure 8: Estimate for modal amplitudes in Mars, assuming that the atmosphere of Mars is exciting the solid body free oscillations by a similar mechanism to the terrestrial continuous free oscillations. Expected amplitudes are at about 30–50 percent of those in the Earth, which may not be impossible to detect but is certainly technically challenging.

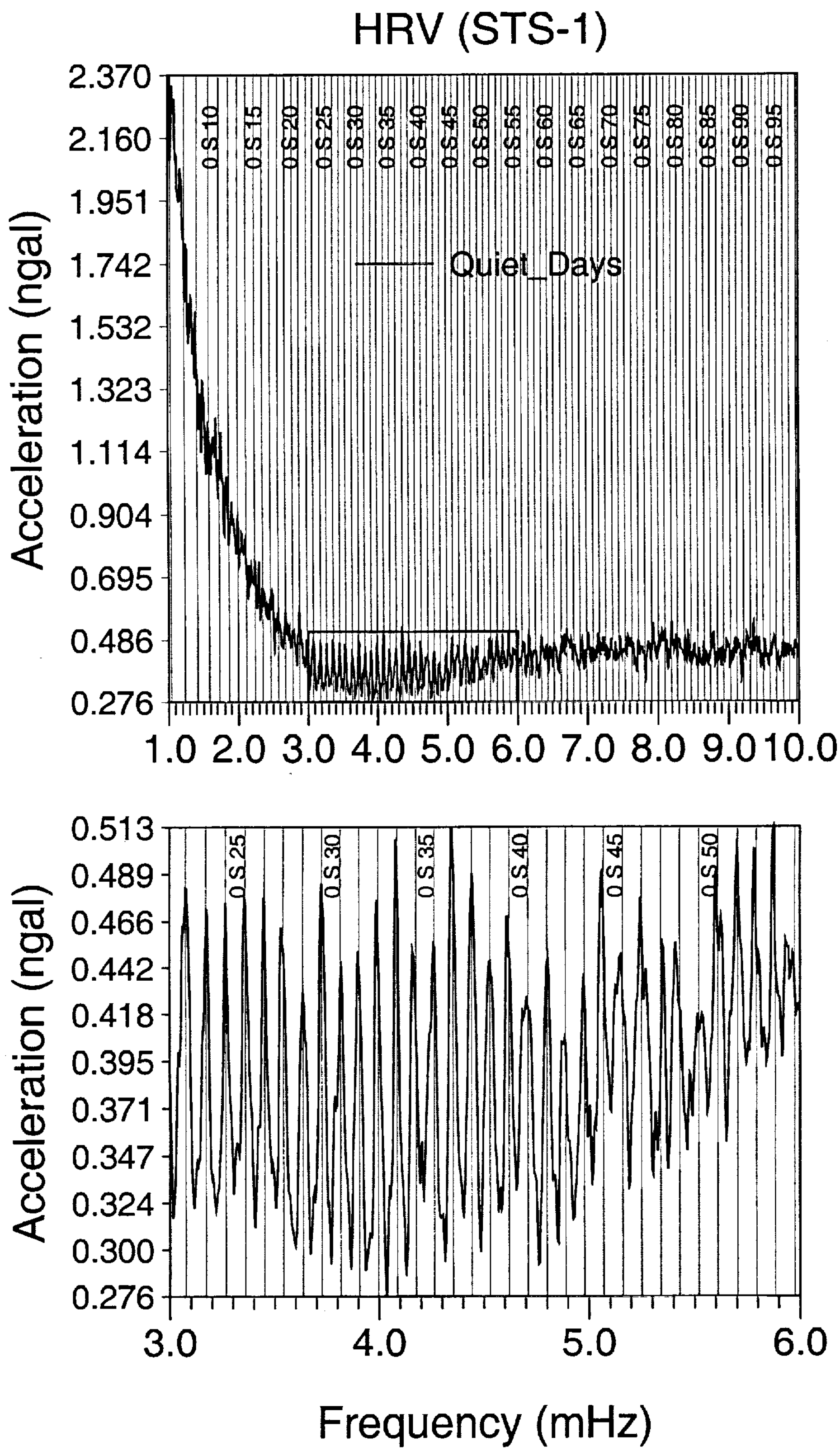
HRV (STS-1)
Acceleration (ngal)
Quiet_Days
0 S 10
0 S 15
0 S 20
0 S 25
0 S 30
0 S 35
0 S 40
0 S 45
0 S 50
0 S 55
0 S 60
0 S 65
0 S 70
0 S 75
0 S 80
0 S 85
0 S 90
0 S 95
2.370
2.160
1.951
1.742
1.532
1.323
1.114
0.904
0.695
0.486
0.276
1.0
2.0
3.0
4.0
5.0
6.0
7.0
8.0
9.0
10.0
Acceleration (ngal)
0.513
0.489
0.466
0.442
0.418
0.395
0.371
0.347
0.324
0.300
0.276
3.0
4.0
5.0
6.0
Frequency (mHz)

Figure 1

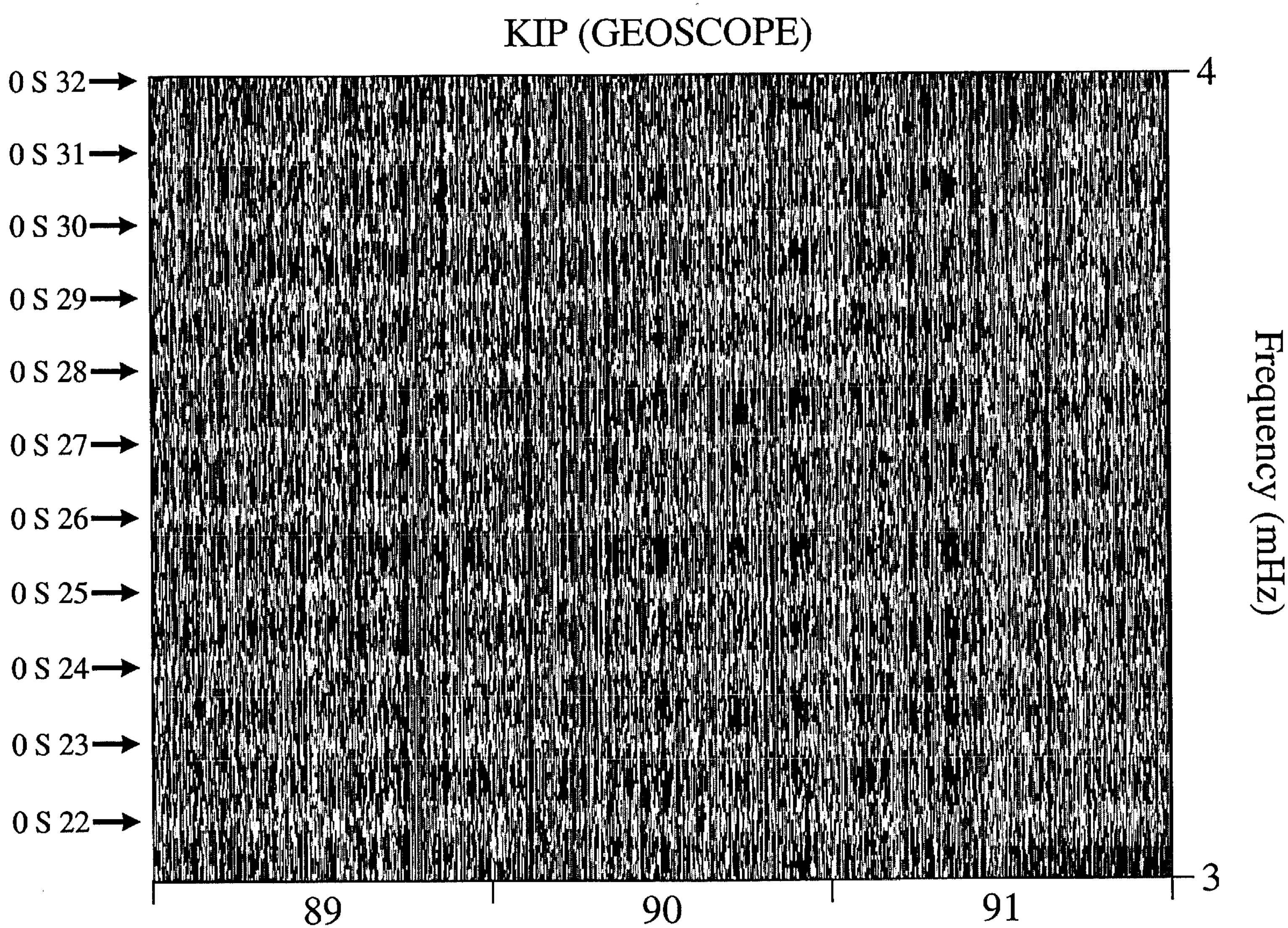

KIP (GEOSCOPE)
0 S 32
0 S 31
0 S 30
0 S 29
0 S 28
0 S 27
0 S 26
0 S 25
0 S 24
0 S 23
0 S 22
4
3
89
90
91
Frequency (mHz)

Figure 2

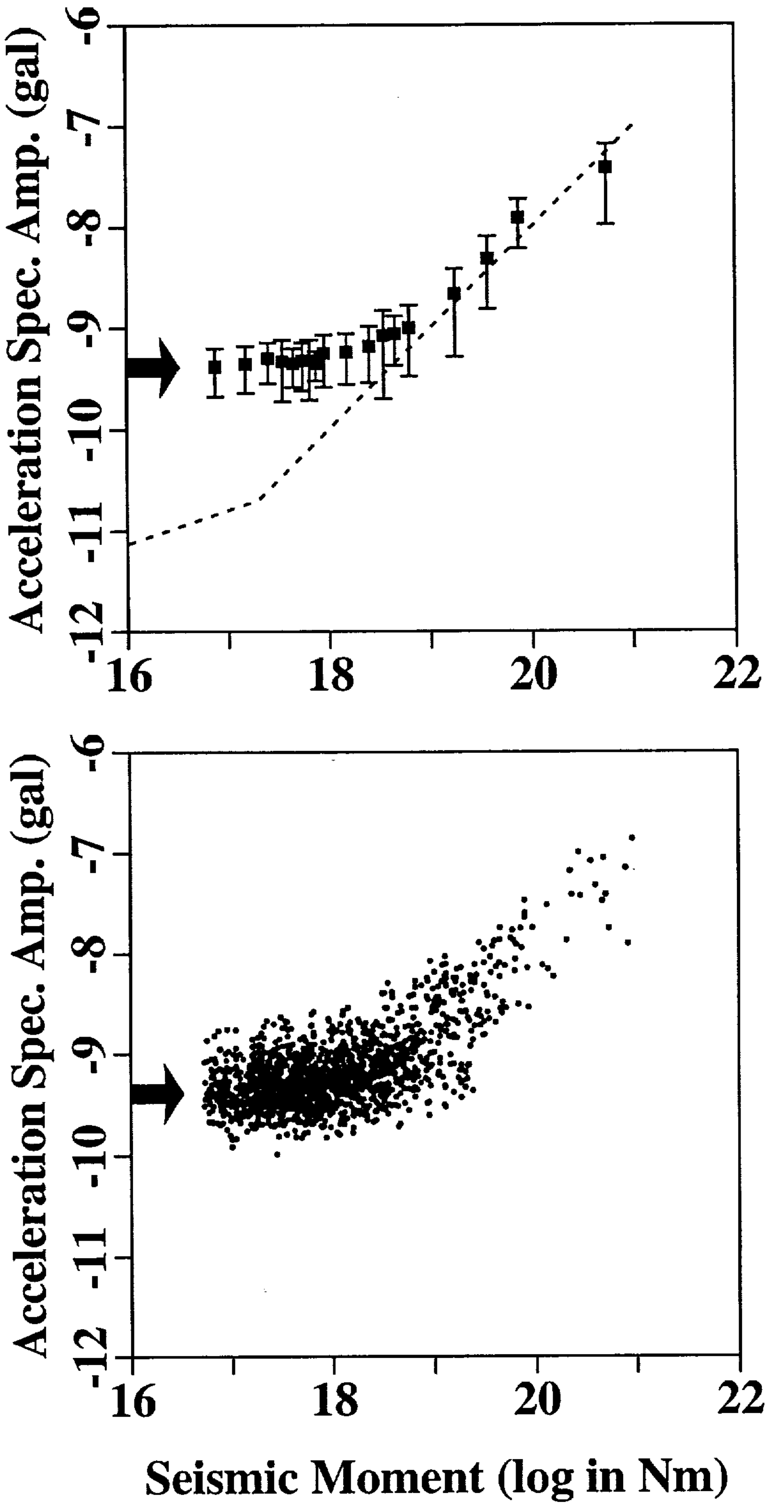
Acceleration Spec. Amp. (gal)
-6
-7
-8
-9
-10
-11
-12
16
18
20
22
Acceleration Spec. Amp. (gal)
-6
-7
-8
-9
-10
-11
-12
16
18
20
22
Seismic Moment (log in Nm)

Figure 3

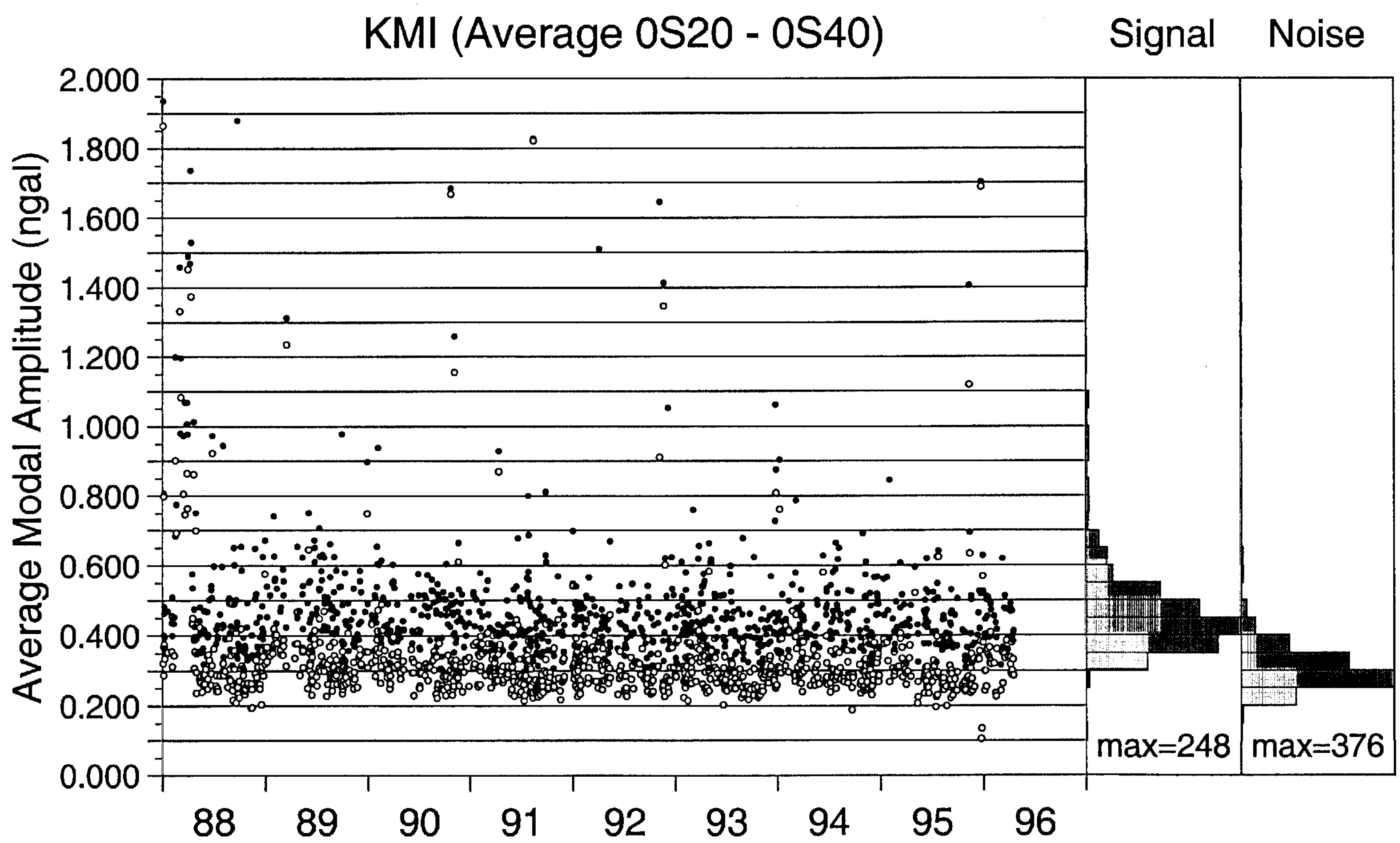
KMI (Average 0S20 - 0S40)
Signal
Noise
Average Modal Amplitude (ngal)
2.000
1.800
1.600
1.400
1.200
1.000
0.800
0.600
0.400
0.200
0.000
88
89
90
91
92
93
94
95
96
max=248
max=376

Figure 4

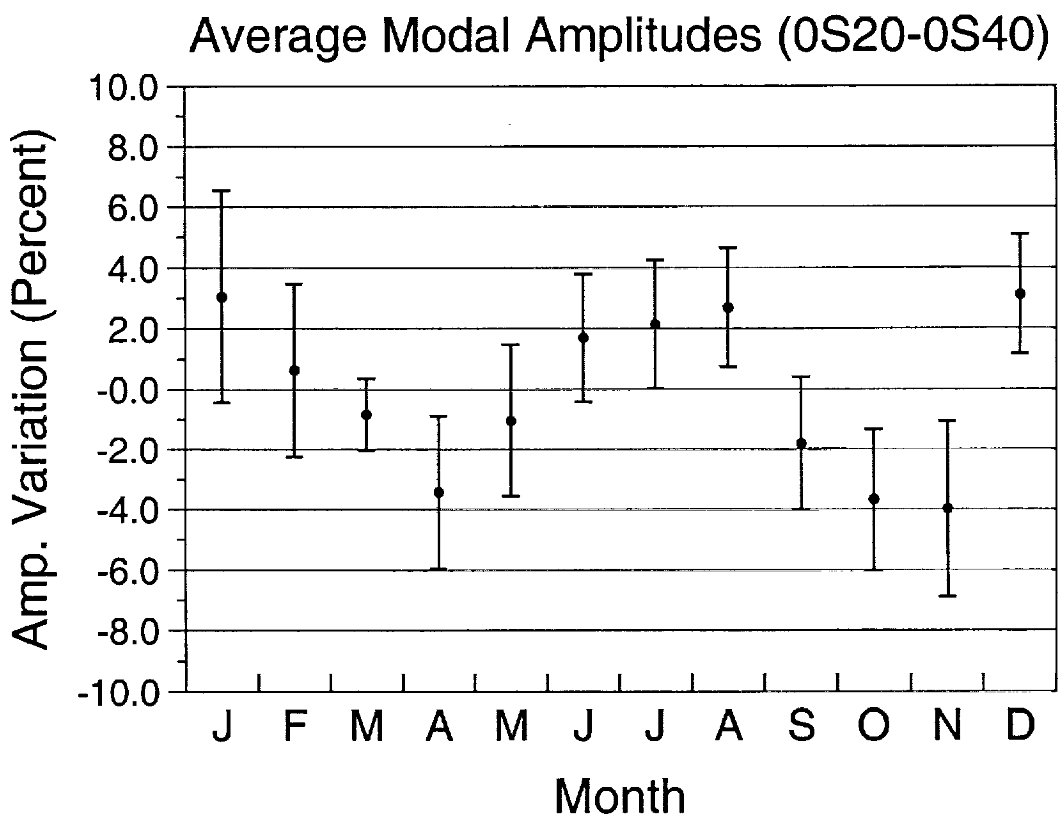
Average Modal Amplitudes (0S20-0S40)
Amp. Variation (Percent)
10.0
8.0
6.0
4.0
2.0
-0.0
-2.0
-4.0
-6.0
-8.0
-10.0
J F M A M J J A S O N D
Month

Figure 5

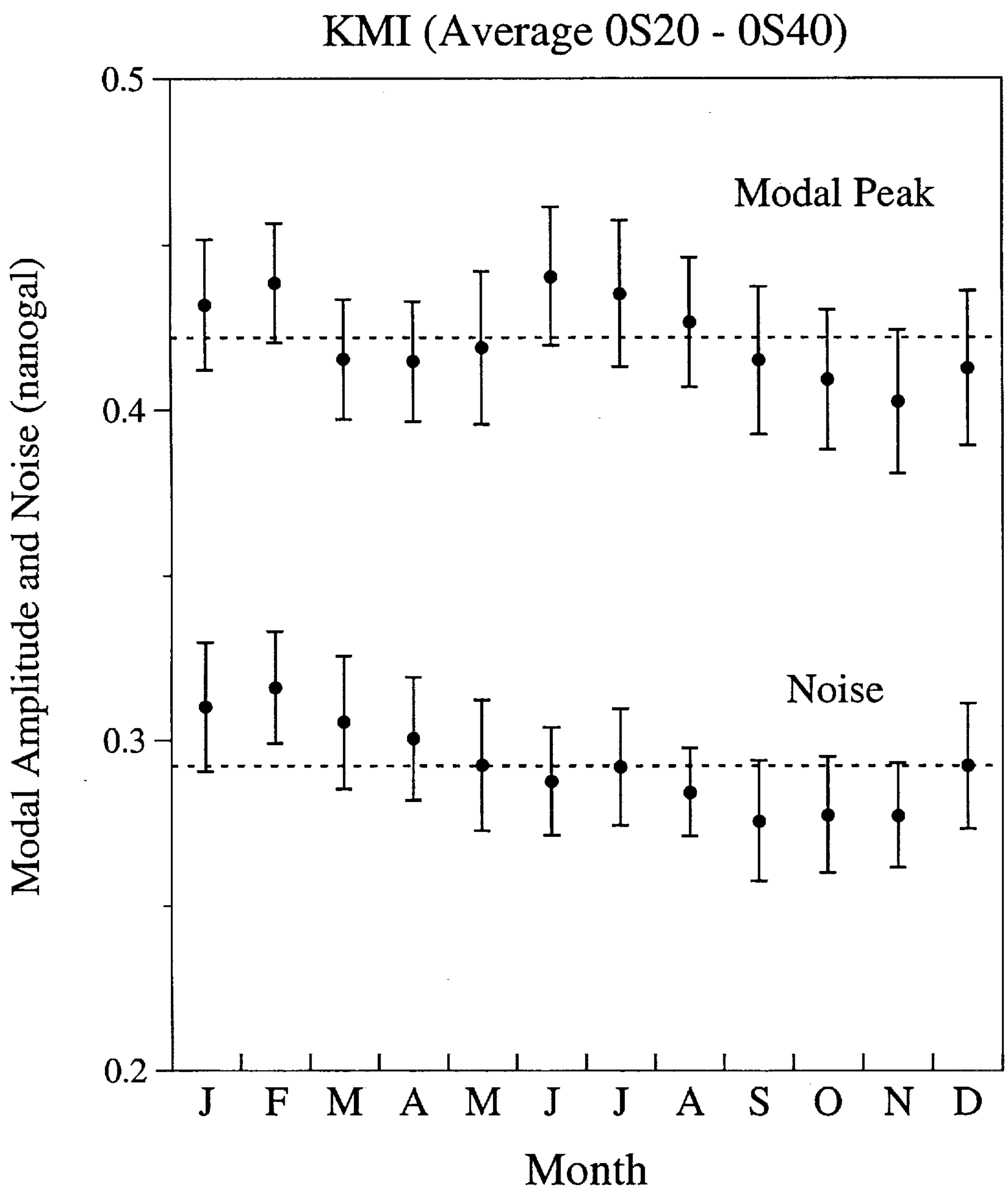

KMI (Average 0S20 - 0S40)
Modal Peak
Noise
Modal Amplitude and Noise (nanogal)
0.5
0.4
0.3
0.2
J
F
M
A
M
J
J
A
S
O
N
D
Month

Figure 6

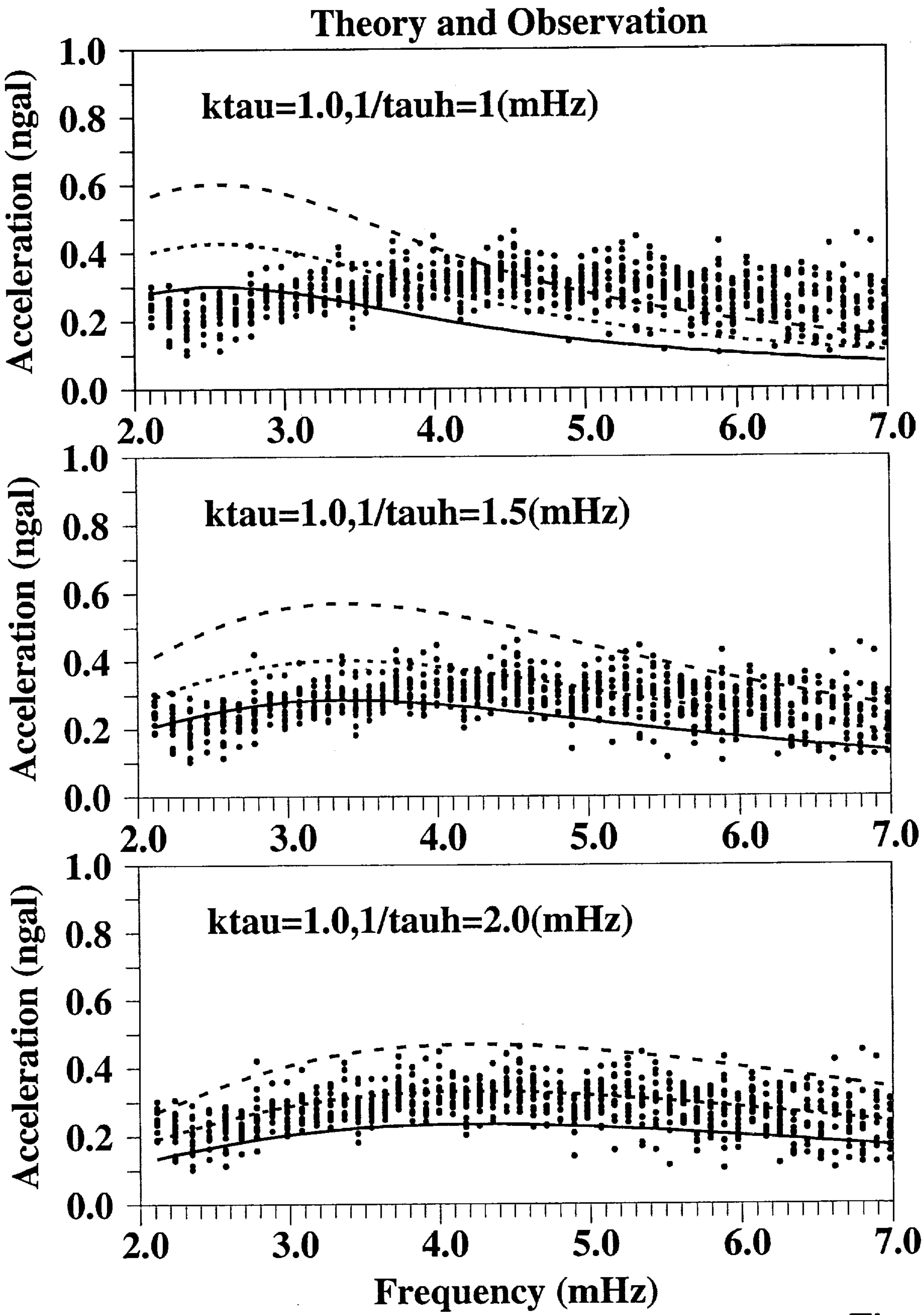
Theory and Observation
ktau=1.0,1/tauh=1(mHz)
ktau=1.0,1/tauh=1.5(mHz)
ktau=1.0,1/tauh=2.0(mHz)
Acceleration (ngal)
Frequency (mHz)
0.0
0.2
0.4
0.6
0.8
1.0
2.0
3.0
4.0
5.0
6.0
7.0

Figure 7

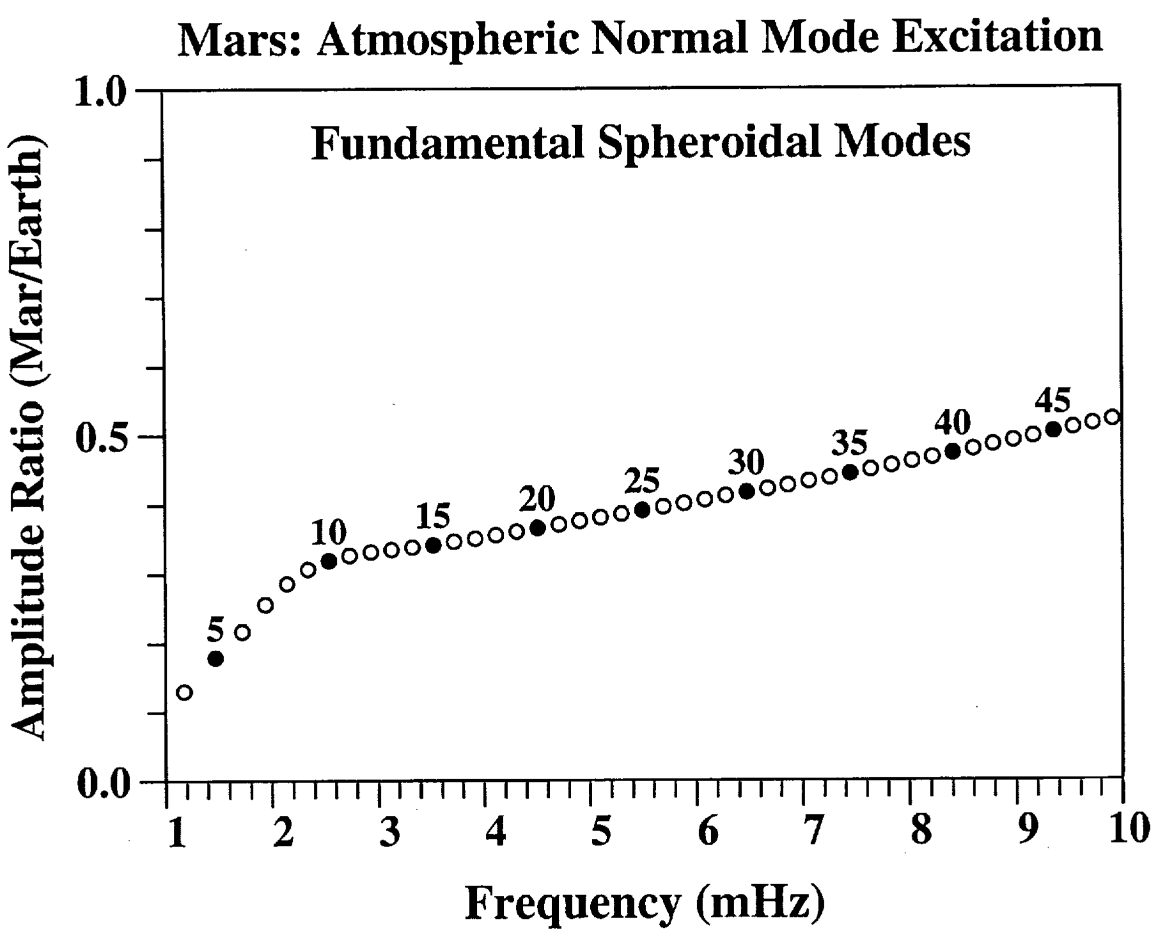
Mars: Atmospheric Normal Mode Excitation
Fundamental Spheroidal Modes
Amplitude Ratio (Mar/Earth)
1.0
0.5
0.0
5
10
15
20
25
30
35
40
45
1
2
3
4
5
6
7
8
9
10
Frequency (mHz)

Figure 8